THE DEVELOPMENT AND APPLICATION OF SCDAP-3D©

E.W. Coryell, L.J. Siefken, and E.A. Harvego

Abstract

The SCDAP-3D© code has been developed at the Idaho National Engineering & Environmental Laboratory (INEEL). The most prominent features of SCDAP-3D© are associated with its linkage to the state-of-the-art thermal/hydraulic analysis capabilities of RELAP5-3D©. Enhancements to the severe accident modeling include the ability to model high burnup and alternative fuel, as well as modifications to support advanced reactor analyses, such as those described by DOE's GenIV initiative. Initial development of SCDAP-3D© is complete and three widely varying but successful applications of the code are summarized. The first application is to a blind calculation of International Standard Problem 45 (ISP-45) or the QUENCH 6 experiment, the second is a large break LOCA analysis performed with an alternative fuel, and the third is an analysis of debris coolability for material that has been relocated to the reactor pressure vessel lower head.

Introduction

The SCDAP-3D© code has been developed from the RELAP5 and SCDAP/RELAP5 codes developed at the Idaho National Engineering & Environmental Laboratory (INEEL) under the primary sponsorship of the U.S. Nuclear Regulatory Commission (NRC). Development of the RELAP5 code series began at the INEEL in 1975, while SCDAP development was initiated in the early 1970's with an active linkage to RELAP5 in 1979. Following the accident at Chernobyl, the U.S. Department of Energy (DOE) began a re-assessment of the safety of its test and production reactors, and chose RELAP5 and SCDAP/RELAP5 as the analytical tools for system safety analysis because of their wide spread acceptance. Systematic safety analyses were performed for the N reactor at Hanford, the K and L reactors at Savannah River, the Advanced Test Reactor (ATR) at INEEL, the High Flux Isotope Reactor (HFIR) and Advanced Neutron Source (ANS) at Oak Ridge, and the High Flux Beam Reactor at Brookhaven. DOE also chose RELAP5 for the independent safety analysis of the New Production Reactor (NPR) before that program was cancelled.

The application of SCDAP/RELAP5 and RELAP5 to these widely varying reactor designs demanded new modeling capabilities, including non-LWR materials and geometry. These widely varying demands were met by maintaining a single source with options that could be selected or deselected at compilation. In this fashion both NRC and DOE users could receive maximum benefit from the others development efforts. After the transmittal of SCDAP/RELAP5 Mod3.3 to the NRC, it became clear, however, that the efficiencies realized by the maintenance of a single source code for use by both NRC and DOE were being overcome by the extra effort required to accommodate sometimes conflicting goals and requirements. The codes were therefore "split" into two versions, SCDAP/RELAP5 Mod3.3 for the NRC and SCDAP-3D© for DOE. The SCDAP-3D© code maintained all of the capabilities and validation history of the predecessor codes, plus the capabilities sponsored by the DOE.

At the outset of the decision to separate the NRC and DOE versions, the INEEL recognized the importance of retaining the pedigree stemming from the extensive validation history of SCDAP/RELAP5. Consequently, the developmental activities have been carefully integrated so as not to compromise this legacy validation. In fact, virtually all of the enhancements to SCDAP-3D© supplement the proven performance and capability of SCDAP/RELAP5.

The most prominent attributes that distinguish SCDAP-3D© from SCDAP/RELAP5 are associated with its linkage to the thermal/hydraulic analysis capabilities of RELAP5-3D©. These features include a fully integrated, multi-dimensional thermal-hydraulic and kinetic modeling capability that removes any restrictions on the applicability of the code to the full range of postulated reactor accidents. Other enhancements include a new matrix solver, new water properties, and improved time advancement for greater robustness.

Enhancements to the severe accident modeling include the ability to model high burnup and alternative fuel, as well as modifications to support advanced reactor analyses, such as those described by DOE's GenIV initiative. Modifications have also been performed to better model analyses of experimental facilities, such as the FZK QUENCH facility, as well as steam generator tube rupture analyses. An interface to the RELAP5-3D© graphical user interface (GUI) has also been added. Together with the modeling capabilities of RELAP5-3D©, these enhancements make the SCDAP-3D© code the most powerful analytical tool of its kind available.

Application of SCDAP-3D© to the QUENCH Facility

One of the most significant measures used in severe accident transient management is the injection of water to cool the uncovered, degraded reactor core. However analysis of the TMI-2 accident and numerous experiments (LOFT, PHEBUS, PBF, CORA, etc.) have shown that before the injected water can cool the core, there will be an enhanced oxidation of the Zircaloy cladding that in turn causes a sharp increase in temperature, hydrogen production, and fission product release. Although the effects of the enhanced oxidation have been observed and accepted, the physical and chemical phenomena have not been well understood. The Forschungszentrum Karlsruhe (FzK) has therefore started an experimental program to:

- Examine the physical and chemical behavior of over-heated fuel elements under various flooding conditions, and
- Examine the effects of water injection at various stages of core degradation, and
- Examine the criteria for cladding failure, oxide layer cracking, and exposure of new metal surface that is currently assumed to result in the temperature escalation.

The QUENCH-06 experiment, performed on December 13, 2000 has been identified as International Standard Problem 45 (ISP-45). This ISP was conducted as a blind standard problem, i.e. only the experimental initial conditions and boundary conditions were given to the participants to perform their calculations, and the results from QUENCH-06, as well as a similar test, QUENCH-05 were kept secret until the delivery date of the calculation results. Although there was no input model and little experience in analyzing the QUENCH facility, the INEEL has used the SCDAP-3D© code to participate in this International Standard Problem.

The QUENCH test facility consists of a test section with electrically heated fuel rod simulators, as shown in Figure 1, a water and steam supply system, an argon gas supply system. Superheated steam from the steam generator and superheater, together with an argon carrier gas, enter the test bundle at the bottom. The effluent, consisting of unconsumed steam, argon, and hydrogen is removed from the top of the bundle, through a water-cooled off-gas pipe, and sent to a condenser. Here the steam is separated from the non-condensable gases, argon and hydrogen, which can then be measured, both by a mass spectrometer and by a "Caldos 7 G" hydrogen detection system.

The test section consists of 21 fuel rod simulators, one unheated instrumentation rod, and twenty electrically heated rods with a heated length of 1024 mm. As shown in Figure 2, the test section is surrounded by a 2.34 mm thick Zircaloy shroud and 36 mm of ZrO_2 fiber insulation. An annular cooling jacket with stainless steel walls surrounds the shroud and insulation. Each heated simulator consists of a 6 mm diameter tungsten heating element surrounded by annular ZrO_2 pellets, a helium gap, and Zircaloy cladding, as shown in Figure 3.

The QUENCH-06 experiment was conducted by first heating the bundle to approximately 900 K in a coolant stream of argon (3 g/s) and steam (3 g/s). The bundle was held at this temperature for about two hours and then ramped to a temperature of approximately 1500 K, and then held at that temperature for about 1 hour to reach the desired oxide thickness. A corner rod was then extracted, to check oxide thickness at that time, and within 5 s, 4 kg of water were injected to rapidly fill the lower parts of the test bundle. At the same time, a quench pump was started to inject water from the bottom of the test section at a rate of ~ 40 g/s. About 20 s later the electrical power was reduced to 4 kW to simulate decay heat. Quenching of the test section was completed within ~250 s, and then steam and electrical power were shut off to terminate the experiment. During the quench phase, argon was injected into the upper plenum to

continue to provide carrier gas for a quantitative hydrogen detection. From the pressure histories at least one rod and the shroud were detected to fail shortly after the initiation of the quench phase. The lowest position of that hole is 0.87 m above the lower end of the heated section. The fiber insulation shows only a slight intrusion of water.

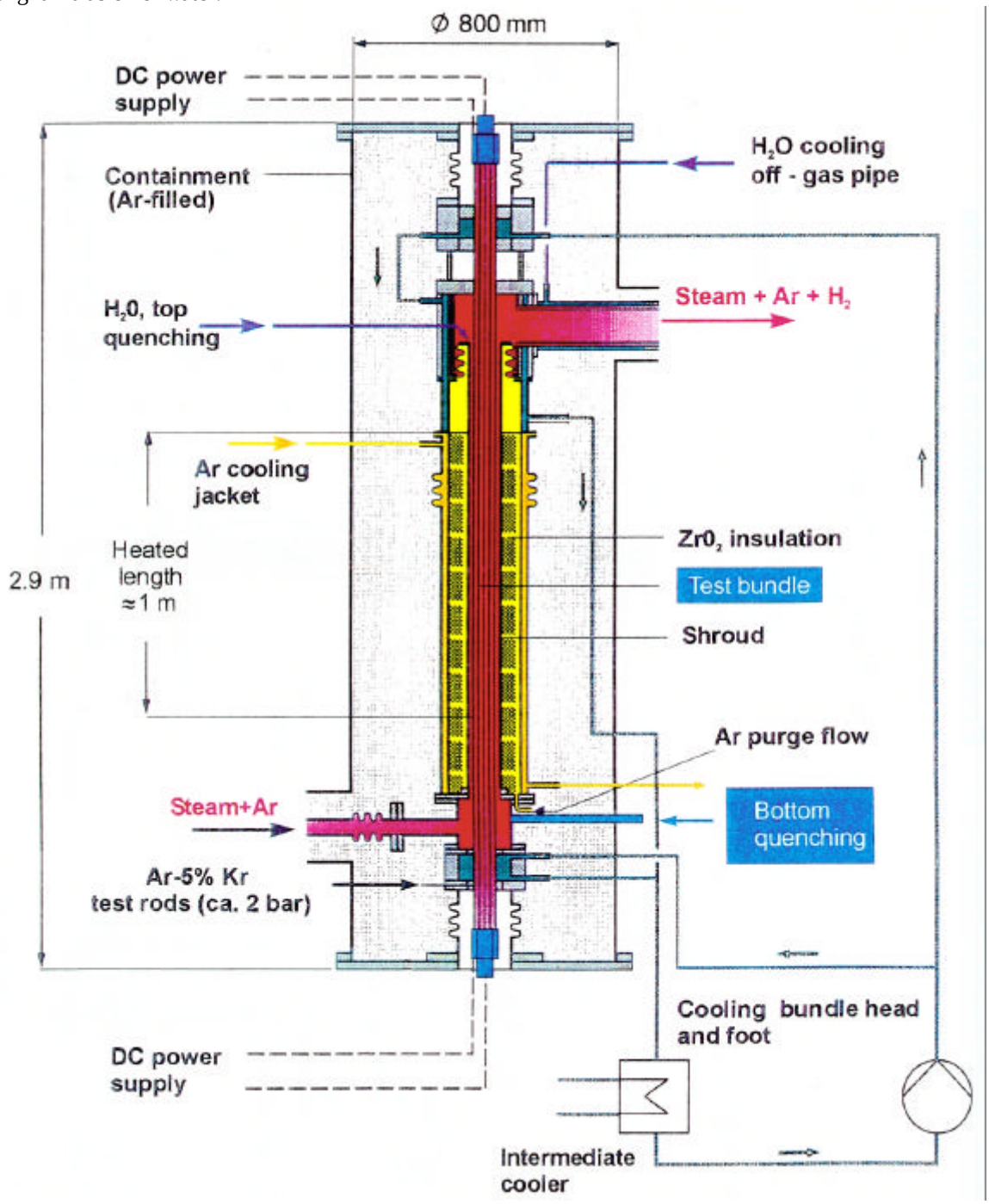

Figure 1 QUENCH Test Facility (courtesy FZK, Hofmann 1998)

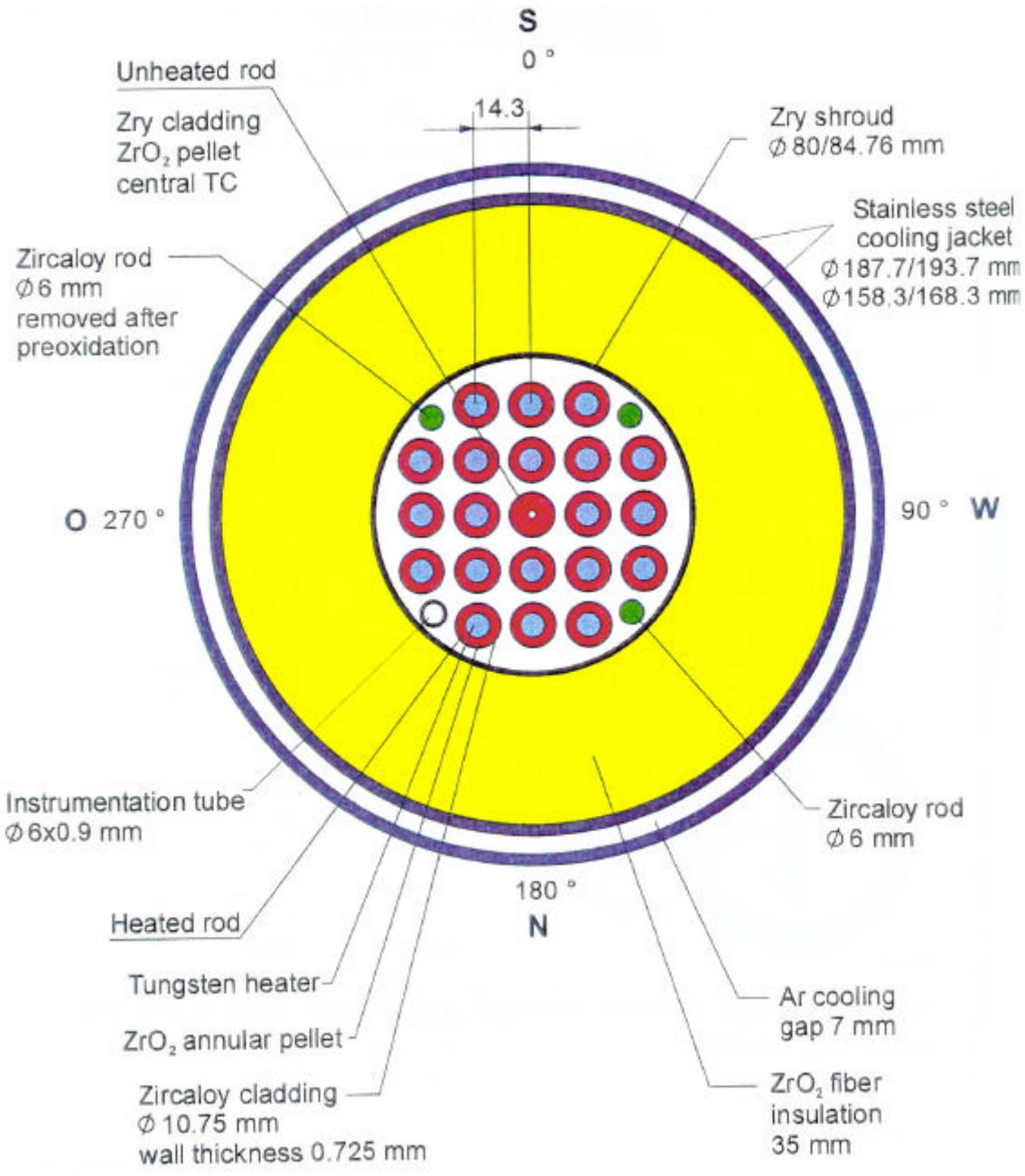

Figure 2 QUENCH bundle configuration (courtesy FZK, Hofmann 1998)

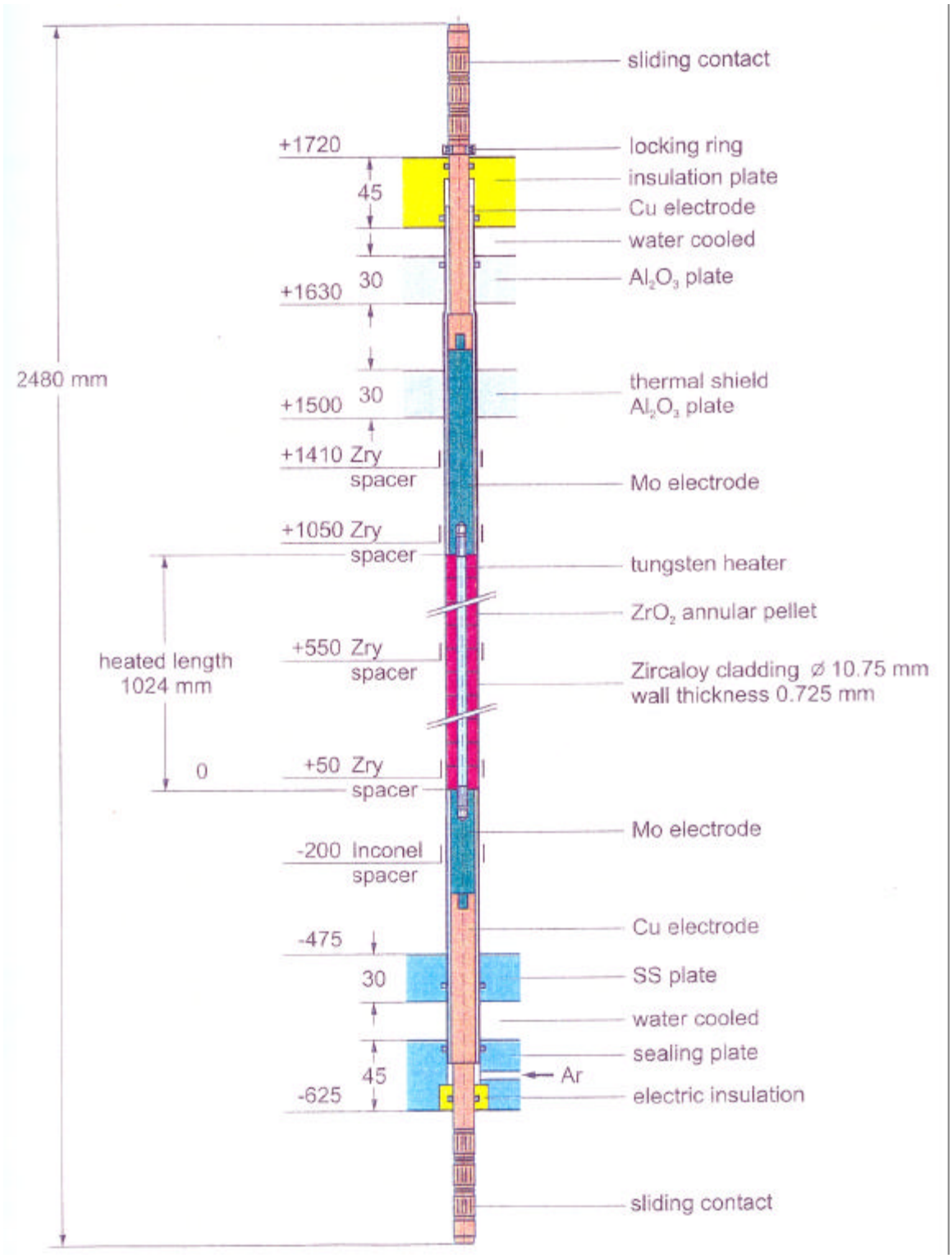

Figure 3 QUENCH fuel rod simulator (courtesy FZK, Hofmann 1998)

Although the experimental data is not yet available, SCDAP-3D© does predict a physically realistic response. Figure 4 shows cladding surface temperatures for a fuel rod simulator during the QUENCH-06 experiment. As shown in this figure, the cladding temperature is initially ramped to the pre-oxidation temperature, and then held at that temperature for approximately an hour. A slow injection of reflood water is then made from the bottom of the bundle. As the lower sections of the bundle begin to quench, they flash sufficient water that nodes in the upper portion of the bundle experience significant additional oxidation. Then as thermal-hydraulic conditions permit, sufficient heat is extracted from the upper portions of the bundle and each axial zone begins to quench, ending the transient.

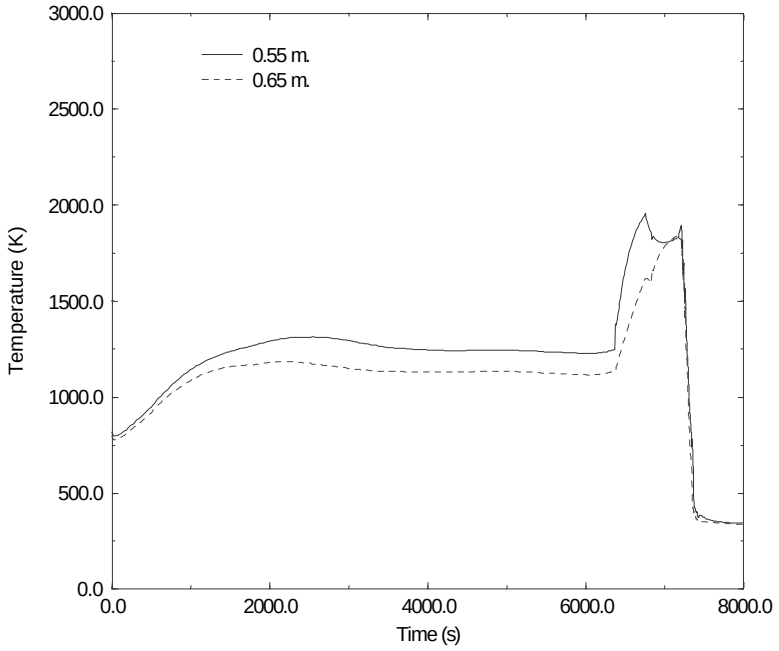

Figure 4 Calculated cladding surface temperatures during QUENCH-06

One of the reasons that the INEEL participated in ISP-45 was to provide an additional assessment of a new Zircaloy oxidation model. This model, first developed for SCDAP/RELAP5 Mod3.3, use an integral diffusion method to calculate oxygen uptake to the cladding, rather than the older parabolic rate equation model. Figure 5 shows the calculated cumulative hydrogen generation for the QUENCH test bundle. As can be seen in this figure, the cladding oxidation produces a significant amount of hydrogen during the initial oxidation period, then levels off until reflood generates the final 60% of the total hydrogen. Although the experimental data has not yet been released by the OECD, this profile seems very realistic and satisfactory. As the data is released, additional comparisons will be performed.

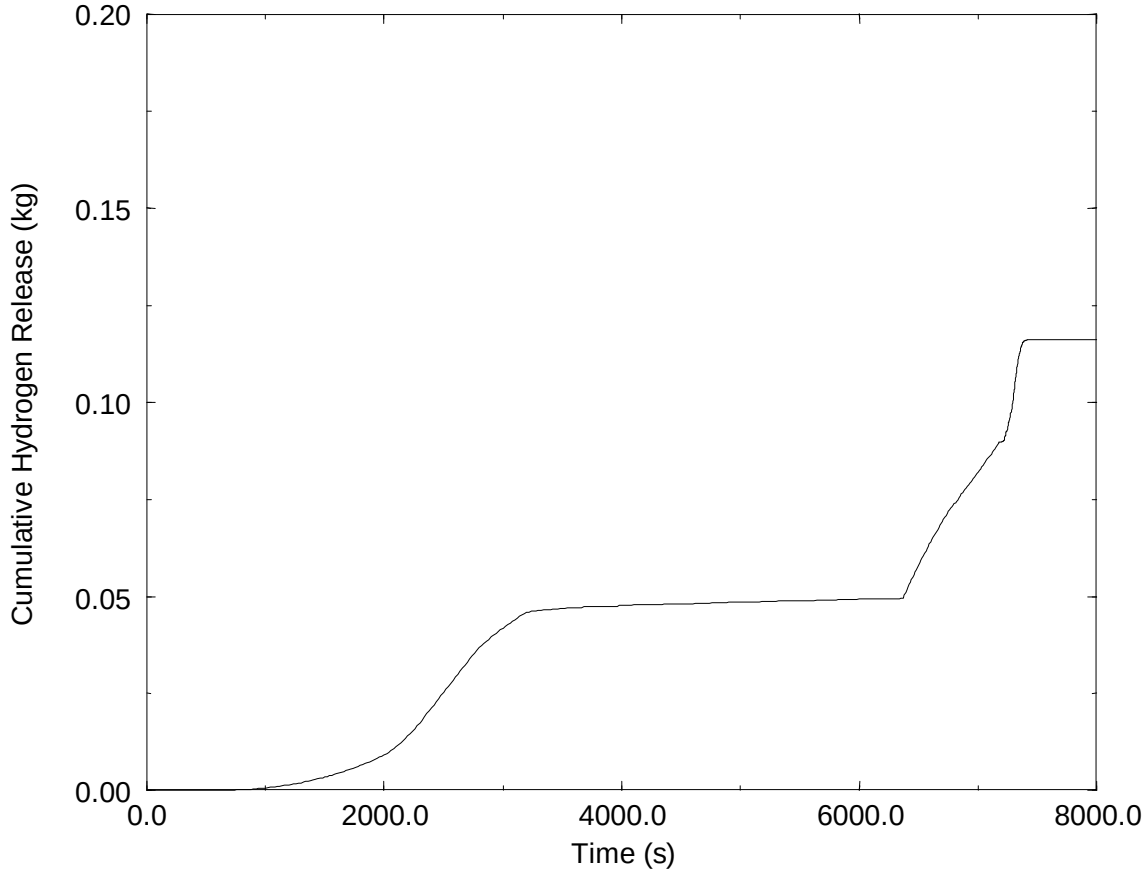

Figure 5 Cumulative hydrogen production during the QUENCH-06 experiment.

Application of SCDAP-3D© to ThO_2-UO_2 Large Break LOCA Analysis

Thoria-urania fuel can be operated to a relatively high burnup level, and may have the potential to improve fuel cycle economics (allow higher sustainable plant capacity factors), improve fuel performance, increase proliferation resistance, and be a more stable and insoluble waste product than traditional UO_2 fuel (MacDonald and Herring 2000). To better understand the impact of this advanced fuel on reactor safety, a large break LOCA analysis has been performed to compare the response of thoria-urania fuel with traditional UO2 fuel.

Although SCDAP-3D© has been successfully applied to large break LOCA analyses for several years, it has been necessary to extend the code to use a mixed thoria-urania fuel in analyses of this type. Extensions were made to allow the code user to describe both high burnup fuel and ThO_2-UO_2 fuel, and material property correlations were added to calculate ThO_2-UO_2 fuel thermal conductivity, heat capacity, density, and emissivity. Other extensions include the ability to model the affect of cladding hydrogen concentration on the behavior of the cladding, and the ability to define the axial distribution in the radial power profile. This addition gives the code the ability to model the large axial variation in radial power peaking factors for fuel rods with high burnup. For example, in a fuel rod with a burnup of 33,000 MWd/MTU the radial peaking factor may vary from 2.0 at the bottom of the fuel rod to 3.0 at the mid-elevation of the fuel rod.

The Seabrook PWR was selected as the framework for comparing the performance of ThO_2-UO_2 and 100% UO_2 fuels during a large break LOCA. This PWR was analyzed in a Nuclear Regulatory Commission sponsored study to evaluate the possibility of relaxing the time to isolate the containment in the event of a large break LOCA (Jones et al. 1992). The Seabrook PWR has four loops in its primary coolant system. During normal power production, the reactor produces 3389 MW of thermal power. The pressure in the

primary coolant system during normal operation is 15.17 MPa (2200 psi). Each coolant loop has a steam generator and a pump. One of the four loops also has a pressurizer. The safety systems on the reactor include an accumulator on each cold leg with the capability to inject 24 m^3 (850 ft^3) of water by nitrogen back pressure when the primary coolant system pressure decreases to value less then 4.14 Mpa. The Seabrook PWR has a core composed of 193 17x17-type fuel assemblies. Except for the composition of the fuel, the characteristics of the fuel assemblies for the ThO_2-UO_2 and 100% UO_2 fuels were identical. The characteristics of the fuel assemblies are described in Table 1. The ThO_2-UO_2 fuel was composed of 70% ThO_2 and 30% UO_2.

Table 1. Characteristics of the fuel assemblies in the Seabrook PWR.

Characteristic	Value
Outer diameter of fuel pellets (mm)	8.19
Outer diameter of fuel rod cladding (mm)	9.50
Thickness of cladding (mm)	0.57
Composition of fuel	100%UO_2 or 70%ThO_2-30% UO_2
Plenum length (m)	0.165
Height of stack of fuel pellets (m)	3.66
Density of fuel (fraction of theoretical maximum)	0.951
Composition of fill gas	100% He
Pressure of fill gas (Mpa)	2.52

The power in the fuel rods was defined according to the Technical Specifications for the Seabrook PWR (Jones et al. 1992). According to these specifications, the average linear heat generation in the reactor core is defined to be 17.83 kW/m and the maximum linear heat generation rate in the reactor core is defined to be a factor of 2.32 greater than the average linear heat generation rate. In addition, the core thermal power is defined to be 102% of its rated thermal power. Thus, the peak linear heat generation rate in the reactor core is 1.02x2.32x17.83 kW/m, which equals 42.19 kW/m. According to the Technical Specifications, the axially averaged linear heat generation in the hottest rod is defined to be a factor of 1.49 greater than the axially averaged average linear heat generation rate in the core. The axial power is defined to have a chopped, symmetric cosine distribution. The ratio of the peak to average linear heat generation in the hottest rod is equal to 1.557, and this ratio for the other rods in the reactor core is defined to be 1.47. The radial power distribution in the reactor core was as follows. The linear power in center four fuel assemblies was a factor of 1.49 greater than the core average linear power. The linear power in the 77 fuel assemblies outward from the center four fuel assemblies was 4.9% greater than the core average linear power. The linear power in the outer 112 fuel assemblies was 94.9% of the core average linear power.

The behavior of the ThO_2-UO_2 and 100% UO_2 fuels at the position of the hottest rod in the reactor core are compared as a function of burnup in Table 2. Although it is highly unlikely that a fuel rod would stay in the position of the hottest fuel rod until an axially averaged burnup of 30,470 MWd/MTU, nevertheless this condition was assumed in order to calculate the earliest possible rupture of fuel rod cladding during a large break LOCA.

Table 2. Comparison of behavior of ThO_2-UO_2 and 100% UO_2 fuel for hottest fuel rod in reactor core

Axially averaged burnup	Centerline temperature at elevation of peak power (K)		Fission gas release (%)		Fuel rod internal pressure (Mpa)	
(MWd/MTU)	100%UO_2	ThO_2-UO_2	100%UO_2	ThO_2-UO_2	100%UO_2	ThO_2-UO_2
870	1904	1921	0.60	0.63	9.02	8.68
10,370	1773	1748	2.14	2.00	9.37	9.00
20,420	1890	1862	10.40	9.49	13.27	12.44
30,470	1996	1958	22.98	20.96	21.73	19.38

The entire primary coolant system of the Seabrook PWR was modeled by SCDAP-3D©. The fluid in the reactor core region was represented by three parallel stacks of nine control volumes, with cross-flow between the stacks taken into account. The first stack of control volumes represented the fluid in the center four fuel assemblies, the second represented the fluid in the 77 fuel assemblies outward from the center four fuel assemblies, and the third represented the fluid in the outer 112 fuel assemblies of the reactor core. The broken loop in the primary coolant system was represented by one network of control volumes and the three unbroken loops were represented by another network of control volumes. The steam generator was represented by eight control volumes, the hot leg by four control volumes, and the cold leg by ten control volumes. Each loop had control volumes to represent a reactor coolant system pump and an accumulator. The broken loop also represented the pressurizer. The reactor vessel downcomer was represented by two parallel stacks of seven control volumes, with cross-flow taken into account. The reactor containment was represented by one control volume.

The large break LOCA was defined to cause a complete, double-ended, offset-shear break in the piping of the cold leg of the coolant system loop with the pressurizer. The Emergency Core Coolant System (ECCS) was assumed to not operate and the primary system coolant pumps are assumed to continue to operate after the initiation of the break.

The transient reactor fission power was calculated using the SCDAP-3D© reactor kinetics model and the transient decay heat was calculated using models appropriate for each composition of fuel. In order to calculate the transient reactor fission power, a table defining reactivity as a function of moderator density was input to the reactor kinetics model. The relation of reactivity to moderator density was assumed to be the same for both compositions of fuel. For the case of 100% UO_2 fuel, the transient decay heat was calculated by the SCDAP-3D© decay heat model. For the case of 70%ThO_2-30%UO_2 fuel, the transient decay heat was obtained from a reactor physics calculation (Herring 2000) and input to the code as a table of power versus time. At 30 s and 60 s after the initiation of the accident, the ratios of decay heat in the 70%ThO_2-30%UO_2 fuel to that in 100% UO_2 fuel were 1.043 and 1.048, respectively.

The performance of the 70%ThO_2-30%UO_2 and 100%UO_2 fuel rods during the large break LOCA were similar. The transient coolant pressure at the center of the reactor core is shown in Figure 6 for the case of 70%ThO_2-30%UO_2 fuel. The transient pressure for the case of UO_2 fuel was similar. The maximum cladding temperatures in the reactor core for the two fuel compositions are compared in Figure 7. For both fuel compositions, the maximum cladding temperatures occurred in the fuel rods with the highest linear fuel rod power and an axially averaged burnup of 30,470 MWd/MTU. In the period from the start of the accident to 34 s after the start of the accident, the cladding temperatures for the two fuel compositions were almost identical. After 34 s, maximum cladding temperature for the 100%UO_2 case was somewhat greater than that for the 70%ThO_2-30%UO_2 case. For both fuel compositions, the heatup of the reactor core was mitigated by the injection of water from the accumulators beginning at 13 s. This injection of water limited the maximum cladding temperature for both cases to a value less than the limit of 1476 K (2200°F) established by the USNRC in 10CFR Part 50.46 (Shotkin et al. 1987). For both fuel compositions, the combination of cladding heatup and depressurization of the primary coolant system was calculated to cause the cladding of some of the fuel rods in the reactor core to balloon and rupture. The time for first rupture of the fuel rod cladding was calculated to be 33 s for both fuel compositions. For both cases, cladding ballooning and rupture was calculated to occur only in the four fuel assemblies in the center of the reactor core.

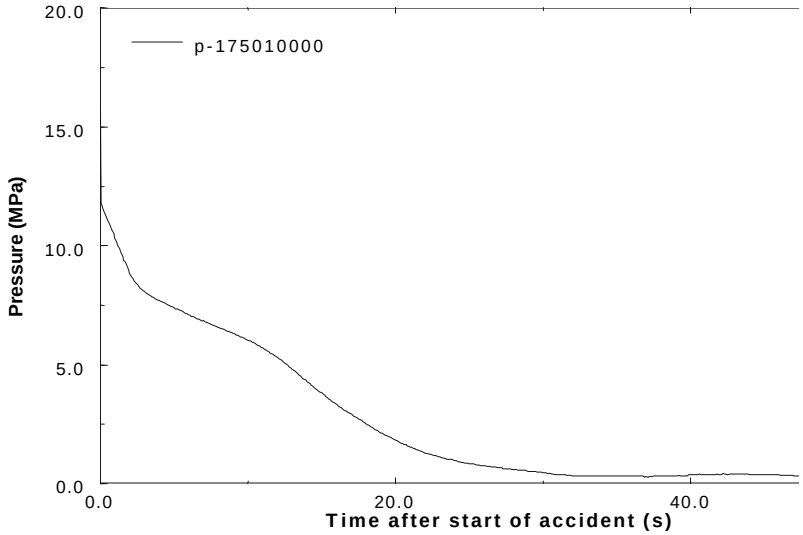

Figure 6. Transient coolant pressure at center of reactor core for case of 70%ThO_2-30%UO_2.

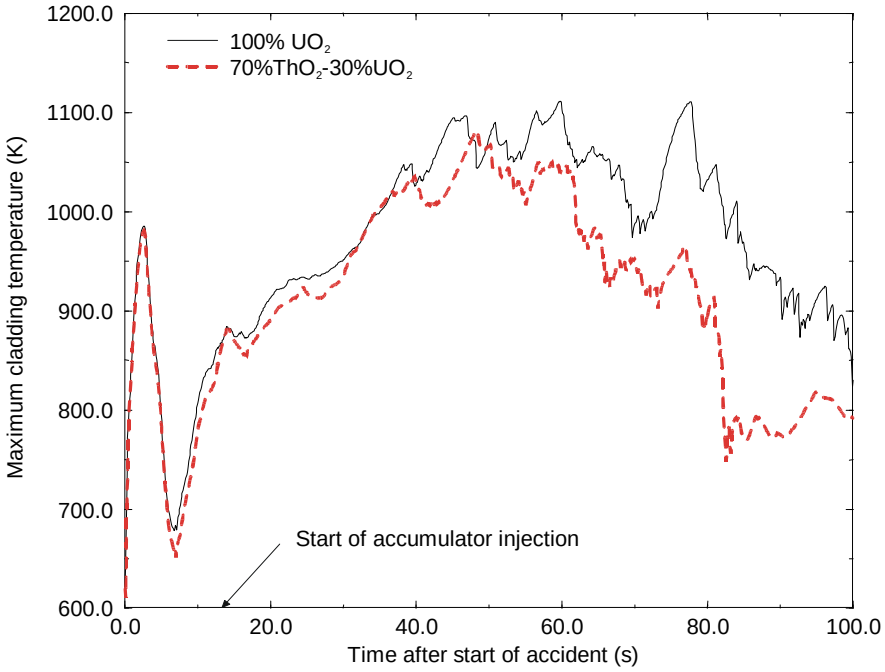

Figure 7. Maximum fuel rod cladding temperature during large break LOCA.

Application of SCDAP-3D© to Debris Coolability Issues

The INEEL has an on-going contract to develop models that describe the heat transfer across the narrow gap between molten core material relocated to the reactor pressure vessel (RPV) lower head and the RPV wall. The presence of this gap, and the heat transfer across it, can be an effective means of cooling the vessel wall thereby preventing RPV failure, as demonstrated by data from the TMI-2, the JAERI ALPHA tests, and the KAERI LAVA experiments.

Comparisons between experimental results and analyses by various codes indicate that, although the initial increase in the vessel wall temperature is well understood, there is insufficient heat loss from the vessel wall after the peak temperature is reached. In the case of SCDAP-3D©, one of reasons for this discrepancy could be that the two-dimensional heat conduction module (COUPLE), used in SCDAP-3D© and other codes, solves the heat conduction equation in a plane geometry for the solid-liquid mixture and the pressure vessel wall. The gap is represented by a NULL element, which is used to calculate the heat flux from debris to wall by conduction across the gap. Functionally, the heat conduction solution method allows only a one-way heat stream. This could cause a higher vessel wall temperature after the initial peak.

INEEL is revising SCDAP-3D© to model the gap as a part of the finite element mesh, with heated surfaces facing the debris and the pressure vessel wall, and to use not only heat conduction, but other heat transfer phenomena as appropriate. The configuration of interest is reflected in Figure 8, which illustrates the relocated core debris filling the pressure vessel lower head, a gap between the solidified debris with counter-current flow within the gap, and the pressure vessel wall. When completed, the revised model will be compared with data from ALPHA tests and, if possible, data from other simulant tests, such as the LAVA tests and the RIT FOREVER tests, and prototypic tests, such as the NUPEC-sponsored COTELS tests. Ultimately, it is hoped that the increased safety margin predicted with this validated model could reduce concerns about ex-vessel phenomena, such as direct containment heating (DCH) and molten core – concrete interaction (MCCI).

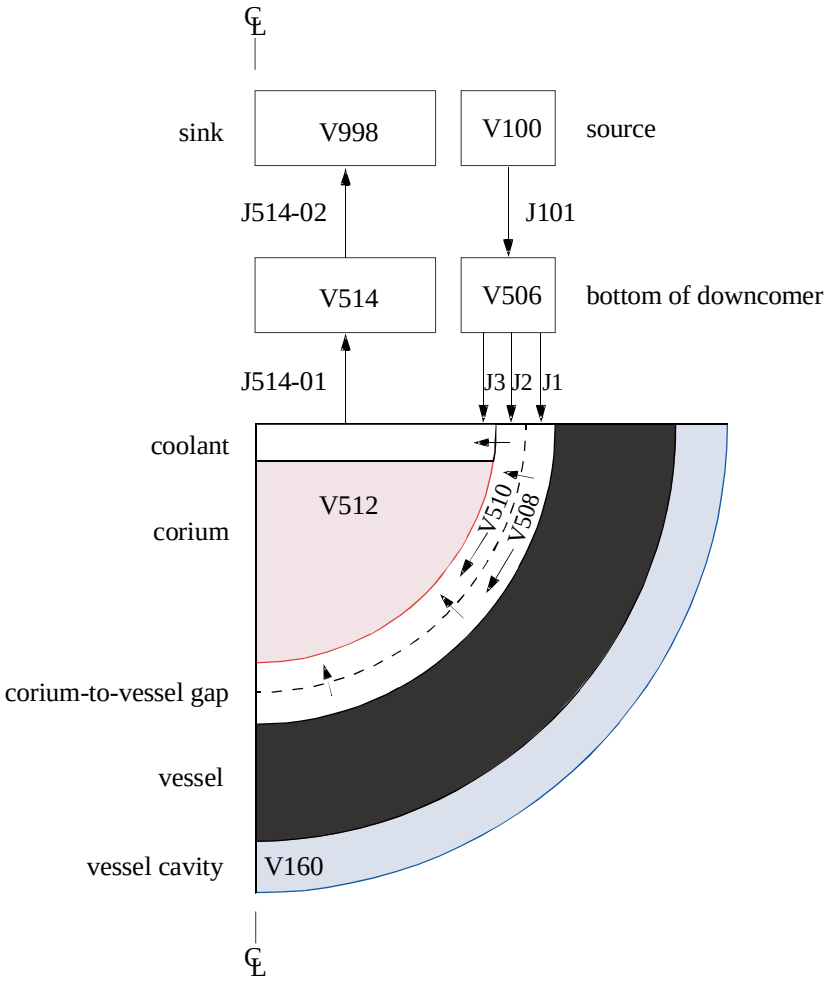

Figure 8. Nodalization diagram for INSS study.

References

SCDAP-3D Code Manual, INEEL-EXT-01-00917, July 2001.

P. Hofmann, W. Hering, C. Homann, W. Leiling, A. Miassoedov, D. Piel, L. Schmidt, L. Sepold, M. Steinbruck, "QUENCH-01 Experimental and Calculational Results", FZKA 6100, November 1998.

W. Hering, CH. Homann, A. Miassodedov, M. Steinbruck, "Specification of the International Standard Problem ISP-45 (QUENCH-06)", OECD/NEA/CSNI/R(2001)1, May 2001

J. Stephen Herring, Personal Communication, September 2000.

K. R. Jones, N. L. Wade, K. R. Katsma, L. J. Siefken., and M. Straka, "Timing Analysis of PWR Fuel Pin Failures," NUREG/CR-5787, EGG-2657, Vol. 1, September 1992.

MacDonald, P. E. and J. Stephen Herring, Advanced Proliferation Resistant, Lower Cost, Uranium-Thorium Dioxide Fuels for Light Water Reactors, 1st Annual Report, 4th Quarterly Report, INEEL/EXT-2000-01217, August 2000.

L. M. Shotkin et al., *Compendium of ECCS Rersearch for Realistic LOCA Analysis*, NUREG-1230, Revsion 4, April 1987.